

Investigation of Sectional Surface Area and Volume of Carpal Tunnel, Median Nerve and Structures Inside in Unilateral Carpal Tunnel Syndrome

Investigación de la Superficie Seccional y el Volumen del Túnel Carpiano, el Nervio Mediano y las Estructuras Internas en el Síndrome del Túnel Carpiano Unilateral

Muhammet Mustafa Gulacti¹; Niyazi Acer²; Hikmet Kocaman³ & Adnan Demirel⁴

GULACTI, M. M.; ACER, N.; KOCAMAN, H. & DEMIREL, A. Investigation of sectional surface area and volume of carpal tunnel, median nerve and structures inside in unilateral CTS. *Int. J. Morphol.*, 42(6):1604-1610, 2024.

SUMMARY: Carpal tunnel syndrome (CTS) is a common entrapment neuropathy of the median nerve (MN). The objective of this study was to evaluate and compare the cross-sectional surface area of the canalis carpi (CC), median nerve (MN), and flexor tendons (FTs) in patients diagnosed with unilateral carpal tunnel syndrome (CTS) with those of the unaffected side, utilizing magnetic resonance imaging (MRI). Additionally, the study aimed to assess and compare the volume of the CC and MN between the affected and unaffected sides. 18 unilateral CTS female patients were included in this study. Magnetic resonance images were obtained using a 1.5-T MRI scanner. The sectional surface area and volume of the CC, MN, and structures inside were measured using Analyze version 12.0 software. The sectional surface area and volume of the CC and MN were significantly larger on the CTS side than on the healthy side ($p < 0.05$). The results showed that the cross-sectional surface area of CC gradually decreased towards the beginning and end of the CC, but the values were higher on the side with CTS than on the healthy side ($p < 0.05$). The cross-sectional surface area of the CC, MN, and FTs was significantly larger on the CTS side compared to the healthy side. Furthermore, the volumes of the CC and MN were notably elevated on the CTS side in comparison to the healthy side. The measurement of these parameters using MRI may be useful in the diagnosis and assessment of CTS.

KEY WORDS: Carpal tunnel syndrome; Magnetic resonance imaging; Carpal tunnel; Median nerve; Volume.

INTRODUCTION

Carpal tunnel syndrome (CTS) is a condition characterized by compression of the median nerve (MN), which is a common entrapment neuropathy (Osiak *et al.*, 2022). The MN traverses from the forearm through the wrist to the hand and is responsible for providing sensation to the palm, thumb, index finger, middle finger, and half of the ring finger. Additionally, it controls certain small muscles in the hand (Löppönen *et al.*, 2022). Compression or constriction of the MN at the wrist can lead to pain, numbness, and tingling in the affected hand and fingers. These symptoms are often triggered by factors such as sleep, repetitive hand or arm positions, and repetitive hand or wrist movements (Osiak *et al.*, 2022). CTS is a prevalent condition that can affect anyone, but is more commonly observed in women and older adults. Repetitive hand and wrist movements, such as typing or using a computer iter, are common causes of CTS. Other conditions,

including arthritis, diabetes, or thyroid disease, can also contribute to its development (Aroori & Spence, 2008; Genova *et al.*, 2020). According to recent studies in the iterature, it is seen that the prevalence and incidence of CTS have increased in recent years, which causes significant socioeconomic costs (Aroori & Spence, 2008; Zhuang *et al.*, 2020).

The pathophysiology of CTS is multifactorial. Increased pressure within the CC is a crucial factor in the development of clinical CTS. Anatomical compression of the MN may result from the increased volume of other components of the CC (Osiak *et al.*, 2022). Fibrosis of the subsynovial connective tissue surrounding the flexor tendons (FTs) may also be a source of compression (Genova *et al.*, 2020). The diagnosis of classical CTS is based on the patient's clinical examination, electromyography (EMG), and nerve conduction

¹ Osmaniye Korkut Ata University, Health Services Vocational School, Osmaniye, Turkey.

² Istanbul Arel University, School of Medicine, Anatomy Department, Istanbul, Turkey.

³ Karamanoglu Mehmetbey University, Faculty of Health Sciences, Department of Physiotherapy and Rehabilitation, Karaman, Turkey.

⁴ Abant İzzet Baysal University Faculty of Medicine, Department of Physical Medicine and Rehabilitation, Bolu, Turkey.

FUNDING. This study was supported by Erciyes University Scientific Research Projects Unit with project number TDK-2015-6250.

studies (Aroori & Spence, 2008). In addition to sensitive electrophysiological tests, there are alternative diagnostic methods for the diagnosis of CTS thanks to the development of new nerve imaging techniques, and there are conservative and surgical treatment methods for its treatment (Hersh *et al.*, 2019).

There are many studies in which measurements of the structures in the canalis carpi (CC) are made by imaging related to CTS (Hersh *et al.*, 2019; Ng *et al.*, 2021; Funahashi *et al.*, 2022). Numerous previous studies on the volume of the CC have reported volumetric differences in CTS compared to healthy individuals (Anderson *et al.*, 2022).

To measure these parameters, various imaging techniques can be used, such as magnetic resonance imaging (MRI), ultrasound (US), and computed tomography (CT) scan. The US is a cost-effective and non-invasive imaging modality that can be used to visualize the CC and MN in real time (Hersh *et al.*, 2019). MRI and CT scan can provide high-resolution images of the CC and surrounding structures, which can be used to accurately measure the sectional surface area and volume (Merhar *et al.*, 1986; Funahashi *et al.*, 2022). MRI is widely accepted as the gold standard for the measurement of peripheral nerve thickness (Crnkovic *et al.*, 2016; Hersh *et al.*, 2019). MRI allows for accurate and detailed visualization of the CC and MN, which is not possible with other imaging modalities like X-ray or ultrasound (Bowers *et al.*, 2022; Öten & Ugur, 2022)

There have been several studies investigating the sectional surface area and volume of the CC, MN, and structures inside in unilateral CTS (Wong *et al.*, 2004; Crnkovic *et al.*, 2016; Bowers *et al.*, 2022; Öten & Ugur, 2022). Wong *et al.* (2004), used US to measure the cross-sectional surface area (CSSA) of the MN proximal to the CC in patients with CTS and compared them to controls. They reported that the CSSA was significantly larger in CTS patients and that it was a useful tool for diagnosing CTS (Wong *et al.*, 2004). Ghasemi *et al.* (2017), used US to measure the CSSA of the MN in patients with CTS and compared them to controls. They reported that the CSSA of the MN was larger in CTS patients and that there was a positive correlation between the sectional area and severity of CTS symptoms (Ghasemi *et al.*, 2017). Crnkovic reported in his study in 2016 that an increase in CC volume was related to an increase in MN CSSA (Crnkovic *et al.*, 2016). Furthermore, MN CSSA has been reported as a prognostic value for CTS and a reliable indicator for disease severity (Ng *et al.*, 2020). However, in CTS, there are limited studies on the volume of MN, and these are controversial (Crnkovic *et al.*, 2012, 2016). Additionally, there have been no studies comparing the volume of the CC and its components between the healthy and CTS side in unilateral CTS.

The objective of this study was to evaluate and compare the cross-sectional surface area of the CC, MN, and FTs in patients diagnosed with unilateral CTS with those of the unaffected side, using MRI. Additionally, the study aimed to assess and compare the volume of the CC and MN between the affected and unaffected sides. This may help to better understand the pathophysiology of CTS and contribute to the development of more effective diagnostic and treatment strategies.

MATERIAL AND METHOD

Study Design. The prospective cross-sectional study included female patients who presented to the Physical Therapy and Rehabilitation clinic at Kahramanmaraş Sutcu Imam University Faculty of Medicine with complaints of hand numbness and weakness, and who were diagnosed with unilateral idiopathic CTS based on their medical history, physical examination, and EMG results. Ethical approval was obtained from the local ethics committee with decision number 2015/424 before the study commenced. The study was conducted in accordance with the Declaration of Helsinki, and written consent was obtained from the female patients included in the study to use their MRI.

Participants. A total of 18 female patients with a diagnosis of CTS and aged between 30-60 years were enrolled in the study. Patients with a history of wrist trauma or surgery, steroid injection, systemic diseases (such as gout and diabetes), kidney disease, and connective tissue disorders such as rheumatoid arthritis were excluded. In the study, demographic information such as age, height, weight, dominant hand, occupational status, number of births, and carpal tunnel questionnaire were recorded for all patients. Diagnosis of CTS was confirmed by both physical examination and EMG, and all patients had CTS on the right side. In addition, all of the patients included in the study had right-sided dominant hands.

Measurements. The proximal and distal margins of the CC were manually determined by using the Analyze 12.0 program on wrist MRI taken routinely at the Radiology Department of KSU Faculty of Medicine. Each measurement was repeated three times, and the results were averaged. The CSSAs of the CC, MN, and FT of nine muscles passing through the CC were measured (Figs. 1 and 2). All measurements were made by the same researcher (MMG).

Volume calculation. Once the boundaries had been delineated for MN and CC, we calculated the volume of each structure by multiplying the area of each slice by the slice thickness and summing the values across all slices.

Volume of MN/CC = $\sum(\text{slice thickness} \times \text{total cross-sectional area of MN/CC})$

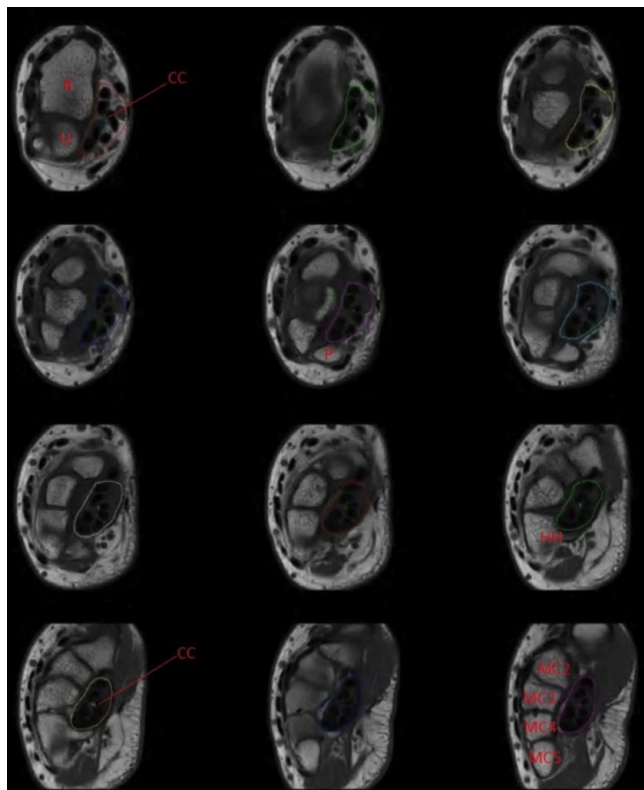


Fig. 1. The CSSAs of the canalis carpi along the carpal tunnel. CC. Canalis carpi; R. Radius; U. Ulna; P. Os pisiforme; HH. Hamulus ossis hamati; MC. Metacarpal.

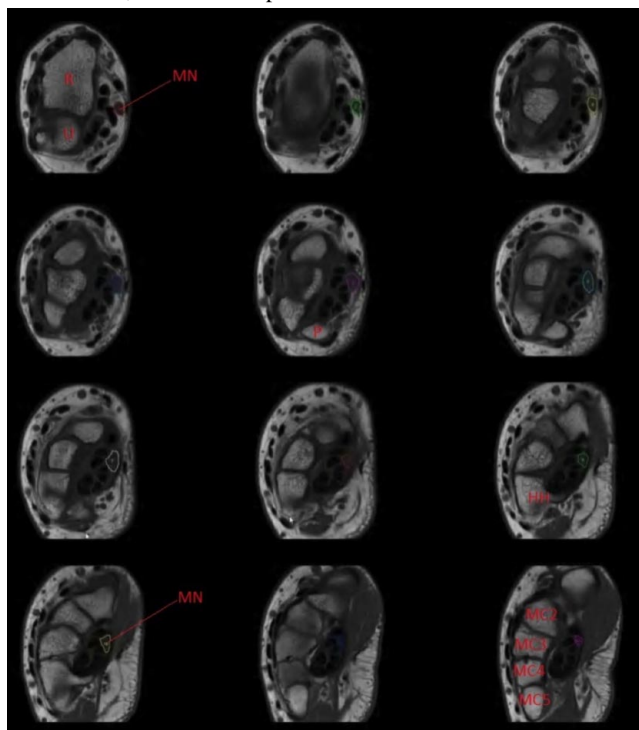


Fig. 2. The CSSAs of the median nerve along the carpal tunnel. MN. Median nerve; R. Radius; U. Ulna; P. Os pisiforme; HH. Hamulus ossis hamati; MC. Metacarpal.

The reference point with the widest CSSA of the CC on the side with CTS was found to be at the level of the radioulnar joint, while the narrowest reference point was the proximal end of the metacarpals. Similarly, the reference point with the largest CSSA of the MN on the side with CTS was found to be the os pisiforme line, with the narrowest reference point being the proximal end of the metacarpals.

MRI sequence. To obtain morphometric data for the CC, images were used from a T1-weighted 1.5 T Philips MRI device. In the determination of the MR acquisition protocol, MRI protocols specified in the literature where the MN images were obtained clearly and the margins were clearly seen were used. The MRI protocol used in this study included fast spin-echo T1-weighted and T2-weighted sequences with a section thickness of 3 mm in the axial plane. The following parameters were used: field of view (FOV) of 100 mm, matrix of 320x320, resolution of 3.2x3.2x3 mm, number of excitations (NEX) of 1, echo train length (ETL) of 2, repetition time (TR) of 543 ms, and time (TE) of 8 ms. T2-weighted images were obtained with a slice thickness of 3 mm in the coronal and axial directions, FOV of 100 mm, matrix of 380 X 380, NEX of 2, ETL of 12, TR of 450 ms, and TE of 11 ms.

Statistical analysis. The collected data was analyzed using SPSS (Statistical Package for the Social Sciences) version 21.0. The normal distribution of the data was assessed using the Kolmogorov-Smirnov test. Descriptive statistics, such as mean and standard deviation, were provided. The independent samples t-test was employed to compare volume and surface area values for variables that exhibited a normal distribution. Pearson correlation analysis was performed to examine the associations between body mass index and the measured values. The statistically significant difference was set as a p-value of $p < 0.05$.

RESULTS

Eighteen female patients between the ages of 30 and 60 with a mean age of 42.11 ± 9.10 years who were diagnosed with CTS were included in the study (Table I).

Table I Demographic data of the individuals participating in the study.

	N	Min.	Max.	Mean \pm SD
Age	18	30	60	42.11 \pm 9.10
Height	18	148	166	160.22 \pm 4.44
Weight	18	57	102	78.00 \pm 10.77
Number of births	18	1	8	3.62 \pm 1.89
BMI	18	24.79	43.80	33.56 \pm 5.16

BMI. body mass index.

Table II. CC, MN and FTs cross-sectional surface area values of patients with CTS and healthy side at four reference points.

Reference point	Side with CTS			Healthy Side		
	CC (mm ²)	MN (mm ²)	FTs (mm ²)	CC (mm ²)	MN (mm ²)	FTs (mm ²)
Distal radioulnar joint	270.49±24.15	18.2±3.1	81.04±9.24	256.26±27.32	15.89±3.1	73.12±10.02
Os pisiforme	216.27±14.95	21.95±4.67	74.01±9.3	194.43±17.22	19.27±3.92	69.21±8.85
Hamulus ossis hamati	186.48±10.46	16.83 ±2.3	79.1±10.23	173.25±16.21	13.86±2.78	72.29 ±9.42
Metacarpus proximal end	176.76 ±9.2	13.86±2.01		169.3±12.73	12.22±2.12	

CTS. Carpal tunnel syndrome; CC. Canalis carpi; MN. median nerve; FTs. Flexor tendons.

In all images related to the MN, it was observed that the CSSA of the MN was the highest at the level of the os pisiforme, and the smallest level was at the level of the distal carpal and the proximal end of the metacarpals (Table II).

When the CC, MN, and FTs CSSAs and the volume values of CC and MN of the healthy individuals and the side with CTS were compared, it was seen that the values were higher than the healthy side without CTS and this was statistically significant ($p < 0.05$, Table III).

Table III Comparison of the measurement values of the individuals participating in the study on the healthy and CTS side.

		Mean	SD	P
CC cross-sectional surface area (mm ²)	With CTS	212.50	14.69	0.015*
	Normal	198.31	18.37	
MN cross-sectional surface area (mm ²)	With CTS	17.71	3.02	0.022*
	Normal	15.31	2.98	
FTs cross-sectional surface area (mm ²)	With CTS	78.08	9.59	0.047*
	Normal	71.54	9.43	
CC volume (mm ³)	With CTS	7965.52	817.28	0.012*
	Normal	7277.93	740.61	
MN volume (mm ³)	With CTS	642.96	113.87	0.019*
	Normal	555.26	98.59	

CTS. Carpal tunnel syndrome; CC Canalis carpi; MN. Median nerve; FTs. Flexor tendons, * $p < 0.05$ (Independent sample t-test).

Table IV shows the correlations between body mass index and CSSAs of the CC, MN, and FTs, as well as CC and MN volume values measured on the side affected by CTS. No statistically significant correlation was observed between body mass index and CSSAs of CC, MN, or FTs ($p > 0.05$). Similarly, there was no significant correlation between body mass index and CC or MN volume values ($p > 0.05$).

Table IV Correlations between body mass index and measurement values on the side with CTS.

		BMI
CC cross-sectional surface area (mm ²)	r	0.094
	p	0.734
MN cross-sectional surface area (mm ²)	r	0.368
	p	0.161
FTs cross-sectional surface area (mm ²)	r	-0.111
	p	0.681
CC volume (mm ³)	r	0.405
	p	0.120
MN volume (mm ³)	r	0.432
	p	0.095

BMI. Body mass index; CC. Canalis carpi; MN. Median nerve; FTs. Flexor tendons; r. Correlation coefficient.

DISCUSSION

In this study, it was observed that the volume of MN and CC in female patients with unilateral CTS was statistically higher compared to the healthy side. Additionally, the CSSAs of the CC, MN, and FTs were significantly larger on the side affected by CTS.

CTS develops due to elevated interstitial pressure in the CC, and mechanical trauma and ischemic injury to the MN play a role in its pathophysiology (Genova *et al.*, 2020; Osiak *et al.*, 2022). While the diagnosis of CTS is mainly based on clinical symptoms, signs, and nerve conduction studies, alternative diagnostic tests such as US and MRI are useful when nerve conduction studies yield normal results (Aroori & Spence, 2008).

MRI reliably display the flexor retinaculum and carpal bones and thus define the boundaries of the CC. MRI is an extremely useful tool for evaluating primary nerve pathologies and space-occupying lesions that cause compression, such as hemangioma, ganglion, or bone deformity, which may affect the range of surgical

interventions (Kumari *et al.*, 2019). The use of MRI as a diagnostic method for CTS has significantly increased in recent years (Ng *et al.*, 2020).

A close association between increasing age and CTS has been reported in the literature, with the highest prevalence occurring between the ages of 40 and 60 (Genova *et al.*, 2020). In the present study, patients diagnosed with CTS had ages ranging from 30 to 60, with a mean age of 42.11 ± 9.10 years. High body mass index (BMI) has also been found to be associated with CTS, with the thickness of the MN cross-section increasing as BMI increases (Bowers *et al.*, 2022; Lampainen *et al.*, 2022). In the present study, the participants had a BMI of 33.56 ± 5.16 , indicating that they were in the risk group for CTS. On the other hand, no significant correlation was found between BMI and CSSAs of CC, MN, or FTs in the current study. This finding may suggest that alterations in CSSAs are not solely attributable to BMI but rather to the presence of CTS.

Wrist positions that are not neutral have been shown to reduce the volume of the CC and compress the MN (Anderson *et al.*, 2022). A study reported that the CC CSSA was 162.4 mm^2 , 175.0 mm^2 , and 173 mm^2 for the 30-degree extension, neutral, and 30-degree flexion positions, respectively (Mogk & Keir, 2008). To enhance the reliability of our findings, MRI was performed in the neutral position. Furthermore, a study by Hersh *et al.* (2019), suggested that MRI and US can serve as alternatives to electromyography and nerve conduction studies for measuring the CSSA of the MN in CTS (

A strong correlation was found between the increased CSSA of the MN and the severity of CTS, as demonstrated in studies using US imaging (Ahmed *et al.*, 2022). Consistent with these findings, our study also identified a differentiation in the cross-section thickness of the MN on the side with CTS. That is, the MN cross-section thickness on the side with CTS was greater than on the healthy side. Multiple studies have reported that individuals with CTS have higher MN CSSAs compared to healthy individuals, particularly at the proximal entrance and distal exit of the CC, as well as at the os pisiforme and hamulus hamati levels (Ng *et al.*, 2020; Bowers *et al.*, 2022). Our study's results align with the existing literature.

In a previous study, it was suggested that MN cross-sectional thickness measurements on MRI could serve as a diagnostic criterion and determine the severity of CTS (Ng *et al.*, 2020). Another study indicated that the CC CSSA gradually decreases from the proximal starting point

to the distal (Merhar *et al.*, 1986; Fujita *et al.*, 2019), which was consistent with our findings. A different study measured the CC CSSA of patients with CTS at the hamulus osis hamati level on MRI as $174.1 \pm 3.7 \text{ mm}^2$ (Fujita *et al.*, 2019). While in our study at the same level, it was $181.39 \pm 15.27 \text{ mm}^2$ on the side with CTS and $173.2 \pm 18.24 \text{ mm}^2$ on the healthy side. Additionally, a recent study conducted in 2021 found that patients with CTS exhibited an increase in CC CSSA on MRI three months after CTS surgery (Ng *et al.*, 2021).

The measurement of the total CSSA of the FTs within the CC is challenging due to tendons displacement. Thus, studies investigating FTs-induced nerve damage and measuring FTs CSSAs are limited (Kunze *et al.*, 2009). In a prior study, the total FTs CSSA was measured as $96.7 \pm 2.6 \text{ mm}^2$ at the osis hamati level in CTS patients, while in the current study, it was measured as $81.04 \pm 9.24 \text{ mm}^2$ (Fujita *et al.*, 2019). The difference in results may be attributed to the fact that only female individuals were included in the current study and demographic differences.

Several studies have measured the volume of the MN following CTS surgery. In a study, it was found that the MN volume increased 90 days after surgery (Crnkovic *et al.*, 2012). Another study measured the CSSA and volume changes of MN after CC release in CTS patients using 3D MRI (Funahashi *et al.*, 2022). In yet another study, the volumes of CC and MN were measured before and after surgery in CTS patients, and significant increases were observed post-surgery (Crnkovic *et al.*, 2016). One study in the literature measured the CC volumes of healthy individuals, mild CTS, moderate CTS, and severe CTS and found a significant difference between the CC volumes of the groups (Öten & Ugur, 2022). In previous studies, the volume changes of the CC and MN in patients with CTS were typically compared before and after surgery. In contrast to previous research, our study compared the CC and MN volumes between the affected side with CTS and the healthy side within the same individuals. Our findings revealed that the CC and MN volumes on the side with CTS were larger compared to those on the unaffected side. In addition, in our study, no correlation was found between BMI and volume values of CC or MN. The absence of correlation between BMI and CC or MN volume values may suggest that alterations in volume are predominantly attributable to the presence of CTS.

In the literature, several studies measured CC volume in CTS patients (Shah & Li, 2020; Peters *et al.*, 2021). Shah & Li (2020), measured the CC volume as 5.367 cm^3 using US on cadavers. In our study, we found that the mean CC volume on the side with CTS was 7.965 ± 0.87

cm³, while it was 7.277 ± 0.74 cm³ on the healthy side. We believe that the difference between our results and those of Shah's study can be attributed to the technology used. CC volume changes in patients diagnosed with CTS have been reported to be different in various studies. The variability in patient BMI and the method used for determining CC CSSAs may contribute to this variability. Furthermore, some studies have compared patients with CTS to healthy individuals, while our study focused on unilateral CTS cases, comparing the healthy and affected sides of the same individuals. As such, our study is original and provides a unique contribution to the literature.

The present study had some limitations. One limitation is that US was not utilized to examine the participants. Generally, US is more convenient and accessible than MRI, providing similar information at a lower cost. Another limitation is the failure to compare electromyography (EMG) and MRI findings, as well as the omission of pain measurement and its association with CTS. Additionally, as CTS typically affects both hands, a primary limitation of our study was the challenge in determining the number of patients with unilateral CTS.

CONCLUSION

In our study, we observed that the CSSAs of CC, MN, and FTs, as well as the volume of CC and MN, were higher on the side with CTS in female patients compared to the healthy side. These findings demonstrate that MRI can be used to accurately measure the carpal tunnel and MN volumes and CSSAs. We believe that clinicians should take into account these observed changes in the wrist affected by CTS when developing treatment plans and evaluating patients in the clinic. By measuring the sectional surface area and volume of the carpal tunnel, MN, and structures inside, clinicians can gain insight into the severity of CTS and the potential for nerve damage. This information can be used to guide treatment decisions, such as the use of conservative therapies (e.g., wrist splints, physical therapy) or more invasive interventions (e.g., corticosteroid injections, surgery).

Overall, investigating the sectional surface area and volume of the carpal tunnel, MN, and structures inside can provide valuable information for the diagnosis, treatment, and monitoring of unilateral CTS.

Ethical Approval

The present study was approved by the Clinical Research Ethics Committee of the Erciyes University Faculty of Medicine (Approved number: 2015/424).

GULACTI, M. M.; ACER, N.; KOCAMAN, H. & DEMIREL, A. Investigación de la superficie seccional y el volumen del túnel carpiano, el nervio mediano y las estructuras internas en el síndrome del túnel carpiano unilateral. *Int. J. Morphol.*, 42(6):1604-1610, 2024.

RESUMEN: El síndrome del túnel carpiano (STC) es una neuropatía por atrapamiento común del nervio mediano (NM). El objetivo de este estudio fue evaluar y comparar la superficie transversal del canal del carpo (CC), el nervio mediano (NM) y los tendones flexores (TF) en pacientes diagnosticados con síndrome del túnel carpiano (STC) unilateral con los del lado no afectado, utilizando imágenes por resonancia magnética. Además, el estudio tuvo como objetivo evaluar y comparar los volúmenes del CC y el NM entre los lados afectados y no afectados. Se incluyeron en este estudio 18 pacientes mujeres con STC unilateral. Las imágenes de resonancia magnética se obtuvieron utilizando un escáner de resonancia magnética de 1,5 T. El área de superficie seccional y el volumen del CC, NM y las estructuras internas se midieron utilizando el software Analyze versión 12.0. El área de superficie seccional y el volumen del CC y del NM fueron significativamente mayores en el lado del STC que en el lado sano ($p < 0,05$). Los resultados mostraron que el área de superficie transversal del CC disminuyó gradualmente hacia el principio y el final del CC, pero los valores fueron mayores en el lado con STC que en el lado sano ($p < 0,05$). El área de superficie transversal del CC, NM y TF fue significativamente mayor en el lado del STC en comparación con el lado sano. Además, los volúmenes del CC y del NM fueron notablemente elevados en el lado del STC en comparación con el lado sano. La medición de estos parámetros mediante resonancia magnética puede ser útil en el diagnóstico y la evaluación del STC.

PALABRAS CLAVE: Síndrome del túnel carpiano; Resonancia magnética; Túnel carpiano; Nervio mediano; Volumen.

REFERENCES

- Ahmed, A.; Malik, G.; Imtiaz, H.; Riaz, R.; Badshah, M. & Zameer, S. Assessment of carpal tunnel syndrome with ultrasonography. *J. Ayub. Med. Coll. Abbottabad.*, 34(2):295-299, 2022.
- Anderson, D. A.; Oliver, M. L. & Gordon, K. D. Carpal tunnel volume distribution and morphology changes with flexion-extension and radial-ulnar deviation wrist postures. *PLoS One*, 17(11):e0277234, 2022.
- Aroori, S. & Spence, R. A. Carpal tunnel syndrome. *Ulster Med. J.*, 77(1):6-17, 2008.
- Bowers, E. M. R.; Como, C. J.; Dooley, S. W.; Morales-Restrepo, A.; Fowler, J. R. Magnetic resonance imaging-measured cross-sectional area of the median nerve. *J. Hand Surg. Glob. Online*, 4(2):93-6, 2022.
- Crnkovic, T.; Bilic, R.; Trkulja, V.; Cesarik, M.; Gotovac, N. & Kolundzic, R. The effect of epineurotomy on the median nerve volume after the carpal tunnel release: a prospective randomised double-blind controlled trial. *Int. Orthop.*, 36(9):1885-92, 2012.
- Crnkovic, T.; Trkulja, V.; Bilic, R.; Gaspar, D. & Kolundzic, R. Carpal tunnel and median nerve volume changes after tunnel release in patients with the carpal tunnel syndrome: a magnetic resonance imaging (MRI) study. *Int. Orthop.*, 40(5):981-7, 2016.
- Fujita, K.; Kimori K.; Nimura, A.; Okawa, A. & Ikuta, Y. MRI analysis of carpal tunnel syndrome in hemodialysis patients versus non-hemodialysis patients: a multicenter case-control study. *J. Orthop. Surg. Res.*, 14(1):91, 2019.

- Funahashi, T.; Suzuki, T.; Hayakawa, K.; Nakane, T.; Maeda, A.; Kuroiwa, T.; Kawano, Y.; Iwamoto, T. & Fujita, N. Visualization of the morphological changes in the median nerve after carpal tunnel release using three-dimensional magnetic resonance imaging. *Eur. Radiol.*, 32(5):3016-23, 2022.
- Genova, A.; Dix, O.; Saefan, A.; Thakur, M. & Hassan, A. Carpal tunnel syndrome: a review of literature. *Cureus*, 12(3):e7333, 2020.
- Ghasemi, M.; Masoumi, S.; Ansari, B.; Fereidan-Esfahani, M. & Mousavi, S. M. Determination of cut-off point of cross-sectional area of median nerve at the wrist for diagnosing carpal tunnel syndrome. *Iran. J. Neurol.*, 16(4):164-7, 2017.
- Hersh, B.; D'Auria, J.; Scott, M. & Fowler, J. R. A comparison of ultrasound and MRI measurements of the cross-sectional area of the median nerve at the wrist. *Hand (N. Y.)*, 14(6):746-50, 2019.
- Kumari, A.; Singh, S.; Garg, A.; Prakash, A. & Sural, S. Tingling hand: magnetic resonance imaging of median nerve pathologies within the carpal tunnel. *Pol. J. Radiol.*, 84:e484-e490, 2019.
- Kunze, N. M.; Goetz, J. E.; Thedens, D. R.; Baer, T. E.; Lawler, E. A. & Brown, T. D. Individual flexor tendon identification within the carpal tunnel: A semi-automated analysis method for serial cross-section MR images. *Orthop. Res. Rev.*, 1:31-42, 2009.
- Lampainen, K.; Shiri, R.; Auvinen, J.; Karppinen, J.; Ryhänen, J. & Hulkkonen, S. Weight-related and personal risk factors of carpal tunnel syndrome in the northern finland birth cohort 1966. *J. Clin. Med.*, 11(6):1510, 2022.
- Löppönen, P.; Hulkkonen, S. & Ryhänen, J. Proximal median nerve compression in the differential diagnosis of carpal tunnel syndrome. *J. Clin. Med.*, 11(14):3988, 2022.
- Merhar, G. L.; Clark, R. A.; Schneider, H. J. & Stern, P. J. High-resolution computed tomography of the wrist in patients with carpal tunnel syndrome. *Skeletal Radiol.*, 15(7):549-52, 1986.
- Mogk, J. P. M. & Keir, P. J. Wrist and carpal tunnel size and shape measurements: effects of posture. *Clin. Biomech.*, 23(9):1112-20, 2008.
- Ng, A. W. H.; Griffith, J. F.; Tong, C. S. L.; Law, E. K. C.; Tse, W. L.; Wong, C. W. Y. & Ho, P. C. MRI criteria for diagnosis and predicting severity of carpal tunnel syndrome. *Skeletal Radiol.*, 49(3):397-405, 2020.
- Ng, A. W. H.; Griffith, J. F.; Tsai, C. S. C.; Tse, W. L.; Mak, M. & Ho, P. C. MRI of the carpal tunnel 3 and 12 months after endoscopic carpal tunnel release. *AJR Am. J. Roentgenol.*, 216(2):464-70, 2021.
- Osiak, K.; Elnazir, P.; Walocha, J. A. & Pasternak, A. Carpal tunnel syndrome: state-of-the-art review. *Folia Morphol. (Warsz.)*, 81(4):851-62, 2022.
- Öten, E. & Uğur, L. 3D volumetric evaluation of the diagnosis and severity of carpal tunnel syndrome using MRI. *J. Clin. Neurosci.*, 97:82-6, 2022.
- Peters, B. R.; Martin, A. M.; Memauri, B. F.; Bock, H. W.; Turner, R. B.; Murray, K. A. & Islur, A. Morphologic analysis of the carpal tunnel and median nerve following open and endoscopic carpal tunnel release. *Hand (N. Y.)*, 16(3):310-5, 2021.
- Shah, R. & Li, Z. M. Ligament and bone arch partition of the carpal tunnel by three-dimensional ultrasonography. *J. Biomech. Eng.*, 142(9):091008, 2020.
- Wong, S. M.; Griffith, J. F.; Hui, A. C.; Lo, S. K.; Fu, M. & Wong, K. S. Carpal tunnel syndrome: diagnostic usefulness of sonography. *Radiology*, 232(1):93-9, 2004.
- Zhuang, T.; Kortlever, J. T.; Shapiro, L. M.; Baker, L.; Harris, A. H. & Kamal, R. N. The influence of cost information on treatment choice: a mixed-methods study. *J. Hand Surg. Am.*, 45(10):899-908, 2020.

Corresponding author:
Muhammet Mustafa Gulacti, PhD
Osmaniye Korkut Ata University
Health Services Vocational School
Osmaniye
TURKEY

E-mail: fztmmgulacti@gmail.com